Approximations of Quantum Corrected Energy-Transport Model with Non-parabolic Energy Relaxation Time

Ren-Chuen Chen
National Kaohsiung Normal University
Department of Mathematics
No.62, Shenjhong Rd., Yanchao Township,
Kaohsiung County 824
TAIWAN (R.O.C.)
rcchen@nknucc.nknu.edu.tw

Jinn-Liang Liu
National Hsinchu University of Education
Department of Applied Mathematics
No. 521, Nanda Rd.,
Hsinchu City 300
TAIWAN (R.O.C.)
jinnliu@mail.nhcue.edu.tw

Abstract: An energy transport model coupled with the density gradient method as quantum mechanical corrections has been proposed and numerically investigated. We called it quantum corrected energy-transport model, QCET model. This model used a parabolic approximation for the energy relaxation time but this is often inadequate to describe advanced semiconductor phenomena. In this paper we extend the QCET model to consider the non-parabolic band diagrams in the sense of Kane. We get explicit expressions of energy relaxation time involving the non-parabolic band effects. An adaptive algorithm for solving this model is applied to solve the problem. Numerical simulations on diodes with the length down to 30 nm using this model have been performed and adaptive meshes are given to demonstrate the accuracy and efficiency of the algorithm. It shows that the energy-band non-parabolicity effect is significant for nano-scale semiconductor devices.

Key–Words: Quantum corrected energy-transport model, Energy-band non-parabolicity, Semiconductor simulation

1 Introduction

For microelectronics, the progress of semiconductor fabrication technology for the advanced metal oxide semiconductor field effect transistor (MOSFET) has been of great interests. The device channel lengths are so small that nonlocal effects become more important for the device characteristics and performance [1, 2, 3, 4]. Semiconductor devices can be simulated by means of the semiconductor Boltzmann equation. However, this method is too costly and time consuming to model real problems in semiconductor applications. Acceptable accuracy can be reached by solving macroscopic semiconductor models which derived from the Boltzmann equation. The simplest models are drift-diffusion models which consist of the mass continuity equation for the charge carriers and a definition for the particle current density [5]. These models, however, are not accurate enough for nano-scale device modelling, owing to the rapidly changing fields and temperature effects [6, 7, 8].

The quantum-corrected energy transport (QCET) model consisting of seven self-adjoint nonlinear partial differential equations (PDEs) describes the steady state of electron and hole flows, their energy transport, and classical and quantum potentials within a nano-scale semiconductor device [9, 10]. Our model is able to explain that electron temperature essentially differs from the lattice temperature. It is clear that this effect cannot be described by the density gradient (DG) model along [11, 12, 13, 14]. Quantum hydrodynamic (QHD) models give accurate simulation results, but the numerical methods to solve this system are too costly and time consuming to model real problems in semiconductor production mode where simulation results are needed in hours or minutes. The QCET model is of parabolic type so that its numerical solution needs less effort than QHD models which contain the hyperbolic nature of the model equations [7, 15, 16].

In this paper, we compute explicitly about the energy relaxation time involving the non-parabolic band effects. For non-parabolic bands in the sense of Kane [7, 17], the coefficients can be computed analytically. We use the Gamma function to compute the energy relaxation time. Moreover, we present the energy relaxation time profiles for both parabolic and non-parabolic band structures.

We assume that the energy-band diagram of the semiconductor crystal is spherically symmetric and monotone in the modulus of the wave vector $\overrightarrow{k}$, that non-degenerate Boltzmann statistics can be used and that a momentum relaxation time τ can be defined by $\tau(\varepsilon) \sim \varepsilon^{-\beta} N(\varepsilon)^{-1}$, where ε is the energy, $N(\varepsilon)$ denotes the density of states, and $\beta > -2$ is a param-

eter. Then, using the general formulas for the coefficients and densities from [6, 18], we get more explicit expressions than those of [6], involving the energy-band function $\varepsilon(\overrightarrow{k})$ and depending on the temperature. Thus, we get analytical expressions under the additional assumption of non-parabolic bands in the sense of Kane.

The paper is divided into the following sections: Section 2 briefly recalls the QCET model considered in [9] and the parabolic energy relaxation time model [19, 20]. A non-parabolic energy relaxation time formulation is then given in Section 3. In Section 4, numerical results of simulation on various diodes to compare with the results in the literature to demonstrate the effectiveness of the proposed model. A short concluding remark is given in Section 5.

2 The Quantum Corrected Energy-Transport Model

As in [9], we consider the following energy-transport model

$$\begin{aligned}
\Delta\phi &= \frac{q}{\varepsilon_s}(n-p+C), && (1)\\
\frac{1}{q}\nabla\cdot\mathbf{J}_n &= R, && (2)\\
\frac{1}{q}\nabla\cdot\mathbf{J}_p &= -R, && (3)\\
\nabla\cdot\mathbf{S}_n &= \mathbf{J}_n\cdot\mathbf{E} - n\left(\frac{\omega_n-\omega_0}{\tau_{n\omega}}\right), && (4)\\
\nabla\cdot\mathbf{S}_p &= \mathbf{J}_p\cdot\mathbf{E} - p\left(\frac{\omega_p-\omega_0}{\tau_{p\omega}}\right), && (5)
\end{aligned}$$

where

$$\begin{aligned}
\mathbf{E} &= -\nabla\phi, && (6)\\
\mathbf{J}_n &= -q\mu_n n\nabla\phi + qD_n\nabla n, && (7)\\
\mathbf{J}_p &= -q\mu_p p\nabla\phi - qD_p\nabla p, && (8)\\
\mathbf{S}_n &= \frac{\mathbf{J}_n}{-q}\omega_n + \frac{\mathbf{J}_n}{-q}k_BT_n + \mathbf{Q}_n, && (9)\\
\mathbf{S}_p &= \frac{\mathbf{J}_p}{+q}\omega_p + \frac{\mathbf{J}_p}{+q}k_BT_p + \mathbf{Q}_p, && (10)\\
\mathbf{Q}_n &= -\kappa_n\nabla T_n, && (11)\\
\mathbf{Q}_p &= -\kappa_p\nabla T_p, && (12)\\
\kappa_n &= 2\left(\frac{k_B}{q}\right)^2 nq\mu_nT_L, && (13)\\
\kappa_p &= 2\left(\frac{k_B}{q}\right)^2 pq\mu_pT_L, && (14)
\end{aligned}$$

and ϕ is the electrostatic potential, q is the elementary charge, ε_s is the permittivity constant of semiconductor, C is the doping profile, n and p are the carrier concentrations, $\mathbf{J}_n$ and $\mathbf{J}_p$ are the carrier current densities, R is the function describing the balance of generation and recombination of electrons and holes, $\mathbf{S}_n$ and $\mathbf{S}_p$ are the energy fluxes for carriers, ω_n and ω_p are the carrier average energies, $\tau_{n\omega}$ and $\tau_{p\omega}$ are the carrier energy relaxation times, $\mathbf{Q}_n$ and $\mathbf{Q}_p$ are the heat fluxes for carries, κ_n and κ_p are carrier conductivities,μ_n and μ_p are the carrier mobilities, D_n and D_p are carrier diffusion coefficients, k_B is Boltzmann's constant and T_n, T_p and T_L are the electron, hole and lattice temperatures.

With the help of the DG model and suitable variable transformation [9] we can obtain the QCET model. The PDEs of the QCET model that govern the carrier transport are then [9]

$$\begin{aligned}
\Delta\phi &= F(\phi,u,v,\zeta_n,\zeta_p), && (15)\\
\frac{1}{q}\nabla\cdot\mathbf{J}_n &= R(\phi,u,v,\zeta_n,\zeta_p), && (16)\\
\frac{1}{q}\nabla\cdot\mathbf{J}_p &= -R(\phi,u,v,\zeta_n,\zeta_p), && (17)\\
\Delta\zeta_n &= Z_n(\phi,u,v,\zeta_n,\zeta_p), && (18)\\
\Delta\zeta_p &= Z_p(\phi,u,v,\zeta_n,\zeta_p), && (19)\\
\nabla\cdot\mathbf{G}_n &= R_n(g_n), && (20)\\
\nabla\cdot\mathbf{G}_p &= R_p(g_p), && (21)
\end{aligned}$$

where

$$\begin{aligned}
F &= \frac{qn_{ie}}{\varepsilon_s}\cdot\left[u\cdot\exp\left(\frac{\phi+\phi_{qn}}{V_T}\right)\right.\\
&\quad \left. - v\exp\left(\frac{-\phi-\phi_{qp}}{V_T}\right)\right] + \frac{q\cdot C}{\varepsilon_s}, && (22)\\
\mathbf{J}_n &= +qD_nn_{ie}\exp\left(\frac{\phi+\phi_{qn}}{V_T}\right)\nabla u, && (23)\\
\mathbf{J}_p &= -qD_pn_{ie}\exp\left(\frac{-\phi-\phi_{qp}}{V_T}\right)\nabla v, && (24)\\
n &= n_{ie}\exp\left(\frac{\phi-\varphi_n+\phi_{qn}}{V_T}\right)\\
&= n_{ie}\exp\left(\frac{\phi+\phi_{qn}}{V_T}\right)u = \zeta_n^2, && (25)\\
p &= n_{ie}\exp\left(\frac{-\phi+\varphi_p-\phi_{qp}}{V_T}\right)\\
&= n_{ie}\exp\left(\frac{-\phi-\phi_{qp}}{V_T}\right)v = \zeta_p^2, && (26)\\
Z_n &= \frac{\zeta_n}{2b_n}\left[V_T\ln(\zeta_n^2)\right.\\
&\quad \left. -V_T\ln(un_{ie}) - \phi\right], && (27)\\
Z_p &= -\frac{\zeta_p}{2b_p}\left[-V_T\ln(\zeta_p^2)\right.\\
&\quad \left. +V_T\ln(vn_{ie}) - \phi\right], && (28)
\end{aligned}$$

$$\phi_{qn} = V_T \ln(\zeta_n^2) - V_T \ln(un_{ie}) - \phi, \quad (29)$$

$$\phi_{qp} = -V_T \ln(\zeta_p^2) + V_T \ln(vn_{ie}) - \phi, \quad (30)$$

$$\mathbf{G}_n = \kappa_n \exp\left(\frac{5\varphi_n}{4V_T}\right) \nabla g_n, \quad (31)$$

$$\mathbf{G}_p = \kappa_p \exp\left(-\frac{5\varphi_p}{4V_T}\right) \nabla g_p, \quad (32)$$

$$R_n = n\left(\frac{\omega_n - \omega_0}{\tau_{n\omega}}\right) - \mathbf{J}_n \cdot \mathbf{E}, \quad (33)$$

$$R_p = p\left(\frac{\omega_p - \omega_0}{\tau_{p\omega}}\right) - \mathbf{J}_p \cdot \mathbf{E}, \quad (34)$$

u and v are the Slotboom variables, n_{ie} is the intrinsic carrier concentration, $\mathbf{G}_n$ and R_n are the rewritten terms for the electron energy transport equation, ϕ_{qn} is the quantum potential and the coefficients $b_n = \frac{\hbar^2}{12m_n^* q}$ is the material parameter measuring the strength of the gradient effects in the gas. For the equation (25) we know that a Maxwell-Boltzmann formula is applied to express the approximation of the carrier concentrations in semiconductors. The important relations and notations are that $V_T = (k_B T_L)/q$ is the thermal voltage, k_B is Boltzmann's constant, φ_n is the generalized quasi-Fermi potential, $u = \exp(\frac{-\varphi_n}{V_T})$, and $\zeta_n = \sqrt{n}$ is a new variable used in the QCET model [9]. In this paper an approximation of R_n with parabolic energy relaxation time is presented as follows:

$$R_n(g_n) = n\left(\frac{\omega_n - \omega_0}{\tau_{n\omega}}\right) - \mathbf{J_n} \cdot \mathbf{E}, \quad (35)$$

where

$$\omega_n = \frac{3}{2} k_B T_n, \quad (36)$$

$\omega_0 = 3/2 k_B T_L$ is the thermal energy, $\tau_{n\omega}$ is expressed by [19, 20]

$$\tau_{n\omega} = \frac{3}{2}\frac{\mu_{n0}}{q v_{sn}^2}\left(\frac{k_B T_n T_L}{T_n + T_L}\right) + \frac{1}{2}\frac{m_n^* \mu_{n0} T_L}{q T_n} \quad (37)$$

μ_{n0} is the low field electronic mobility, v_{sn} is the electron saturation velocity, m_n^* is the effective electron mass and g_n is the Slotboom-like variable defined by

$$T_n = g_n \exp\left(\frac{5\varphi_n}{4V_T}\right). \quad (38)$$

We note that there are another expressions for the electron energy flux. Substituting (7), (11), (13) and (25) into (9) we obtain

$$\mathbf{S}_n = -\frac{5}{2}\frac{\mathbf{J}_n}{q} k_B T_n - \kappa_n \nabla T_n, \quad (39)$$

$$= \frac{5}{2} k_B \mu_n T_n (n \nabla \phi) - \frac{5}{2} k_B D_n (T_n \nabla n) - \kappa_n \nabla T_n. \quad (40)$$

3 A Non-parabolic Energy Relaxation Time

In this section we reformulate the energy relaxation time for the QCET model and make four important assumptions as in [6]:

(H1) The energy-band diagram ε of the semiconductor crystal is spherically symmetric and a strictly monotone function of the modulus $k = |\overrightarrow{k}|$ of the wave vector $\overrightarrow{k}$.

(H2) A momentum relaxation time can be defined by

$$\tau(\epsilon) = \left(\phi_0(2N_0 + 1)\varepsilon^\beta N(\varepsilon)\right)^{-1}, \quad \beta > -2, \quad (41)$$

where $N(\varepsilon)$ is the density of states of energy $\varepsilon = \varepsilon(k)$.

(H3) The electron density n and the internal energy E are given by non-degenerate Boltzmann statistics.

(H4) The relation for non-parabolic bands in the sense of Kane [6] is defined as follows,

$$\varepsilon(1 + \alpha\varepsilon) = \frac{k^2}{2m^*}, \quad (42)$$

where m^* is the (scaled) effective electron mass given by $m^* = m_0 k_B T_L/\hbar^2 k_0^2$, and $\alpha > 0$ is the (scaled) non-parabolicity parameter. Notice that we get a constant energy relaxation time if $\alpha = 0$.

Under these assumptions, the (scaled) temperature-dependent energy relaxation time model can be written as [6]

$$\tau_\beta(T_{ns}) = \tau_0 \frac{3q(\alpha T_{ns}, 0)}{2r_\beta(\alpha T_{ns})} T_{ns}^{1/2-\beta} \quad (43)$$

where $T_{ns} = T_n/T_L$ is the scaled electron temperature, τ_0 is the energy relaxation time constant, i.e., 0.4×10^{-12} seconds used in this paper, r_β is

$$r_\beta(\alpha T) = \int_0^\infty (1 + \alpha T u)(1 + 2\alpha T u)^2 u^{1+\beta} e^{-u}\, du, \quad (44)$$

and $q(\alpha T, l)$ is

$$q(\alpha T, l) = \int_0^\infty (1+\alpha T u)^{1/2}(1+2\alpha T u) u^{1/2+l} e^{-u}\, du. \quad (45)$$

In the physical literature, the values $\beta = 1/2$ (used by Chen et al. [7]) and $\beta = 0$ (used by Lyumkis et al. [8]) have been used in the case of parabolic and

non-parabolic band structure. By the notations in [6] we know that the scaled stationary energy-transport model reads as follows:

$$\begin{aligned}
\lambda^2 \triangle \phi_s &= n_s - C_s, && (46)\\
-\nabla \cdot \mathbf{J}_{ns} &= 0, && (47)\\
-\nabla \cdot \mathbf{S}_{ns} &= -\mathbf{J}_{ns} \cdot \nabla \phi_s + W_{ns}, && (48)\\
\mathbf{J}_{ns} &= \nabla(\mu_\beta^{(1)} T_{ns} n_s) - \mu_\beta^{(1)} n_s \nabla \phi_s, && (49)\\
\mathbf{S}_{ns} &= \nabla(\mu_\beta^{(2)} T_{ns}^2 n_s) - \mu_\beta^{(2)} T_{ns} n_s \nabla \phi_s, && (50)
\end{aligned}$$

where the similar dimensionless quantities marked by the subscript s,

$$\mu_\beta^{(i)} = \mu_0 \frac{p_\beta(\alpha T_{ns}, i+1)}{q(\alpha T_{ns}, 0)} T_{ns}^{-1/2-\beta}, \quad i = 1, 2, \tag{51}$$

μ_0 is the low-field mobility constant, i.e., 1.5×10^3 cm^2 V^{-1} s^{-1} used in this paper, and

$$p_\beta(\alpha T, l) = \int_0^\infty \frac{1 + \alpha T u}{(1 + 2\alpha T u)^2} u^{l-\beta-1} e^{-u}\, du. \tag{52}$$

Consider the case $\alpha = 0$ and $\beta = 1/2$.

$$\begin{aligned}
q(0,0) &= \int_0^\infty u^{1/2} e^{-u}\, du,\\
p_{1/2}(0,2) &= \int_0^\infty u^{1/2} e^{-u}\, du,\\
p_{1/2}(0,3) &= \int_0^\infty u^{3/2} e^{-u}\, du.
\end{aligned}$$

Let the symbol Γ denotes the Gamma function defined by

$$\Gamma(s) = \int_0^\infty u^{s-1} e^{-u}\, du, \quad s > 0.$$

We know that $\Gamma(3/2) = \sqrt{\pi}/2$, $\Gamma(5/2) = 3\sqrt{\pi}/4$ and $\Gamma(7/2) = 15\sqrt{\pi}/8$. We obtain

$$\begin{aligned}
q(0,0) &= \frac{1}{2}\sqrt{\pi}, && (53)\\
p_{1/2}(0,2) &= \frac{1}{2}\sqrt{\pi},\ p_{1/2}(0,3) = \frac{3}{4}\sqrt{\pi}, && (54)\\
\mu_{1/2}^{(1)} &= \mu_0 T_s^{-1},\ \mu_{1/2}^{(2)} = \frac{3}{2}\mu_0 T_s^{-1}, && (55)\\
\mathbf{S}_{ns} &= -\frac{3}{2}\mu_0 \nabla(T_s n_s) + \frac{3}{2}\mu_0 n_s \nabla \phi_s,\\
&= -\frac{3}{2}\mu_0 (T_s \nabla n_s) - \frac{3}{2}\mu_0 (n_s \nabla T_s)\\
&\quad + \frac{3}{2}\mu_0 (n_s \nabla \phi_s). && (56)
\end{aligned}$$

Comparing (40) and (56) we know that the QCET model is the same structure as the model used by Chen et al. with model parameter β = 1/2. Thus, we only consider the case $\beta = 1/2$. A first-order approximation can be obtained as follows,

$$\begin{aligned}
r_{1/2}(\alpha T) &\doteq \int_0^\infty (1 + 5\alpha T u) u^{3/2} e^{-u}\, du,\\
&= \int_0^\infty u^{3/2} e^{-u}\, du + 5\alpha T \int_0^\infty u^{5/2} e^{-u}\, du\\
q(\alpha T, 0) &\doteq \int_0^\infty (1 + \frac{5}{2}\alpha T u) u^{1/2} e^{-u}\, du.\\
&= \int_0^\infty u^{1/2} e^{-u}\, du + \frac{5}{2}\alpha T \int_0^\infty u^{3/2} e^{-u}\, du
\end{aligned}$$

So the scaled energy relaxation time model can be approximated by

$$\tau_{1/2}(T) = \tau_0 \frac{12 + 45\alpha T}{12 + 150\alpha T} \tag{57}$$

and the unscaled one is

$$\tau_{1/2}(T_n) = \tau_0 \frac{12T_L + 45\alpha T_n}{12T_L + 150\alpha T_n} \tag{58}$$

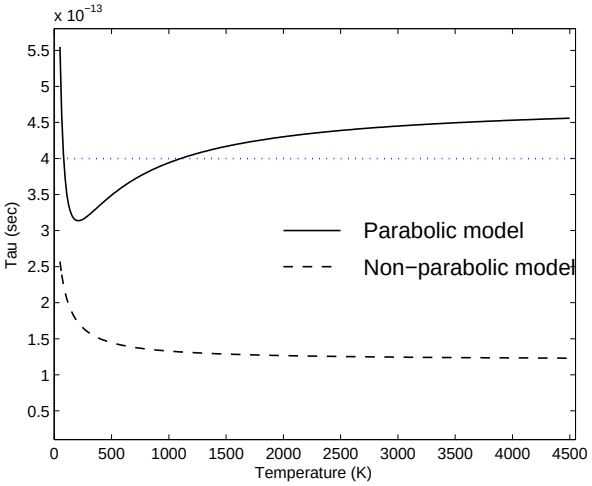

Figure 1: Parabolic and non-parabolic energy relaxation time models.

Fig. 1 shows the behaviors of the parabolic and non-parabolic energy relaxation time models where $\tau_0 = 0.4 \cdot 10^{-12} s$ [6]. The energy balance equation with non-parabolic energy relaxation time is

$$\begin{aligned}
&\nabla \cdot \left(\kappa_n \exp(\frac{5\varphi_n}{4V_T}) \nabla g_n \right)\\
&= \frac{3}{2} \cdot \frac{k_B n \left(g_n \exp(\frac{5\varphi_n}{4V_T}) - T_L \right)}{\tau_0 \frac{12T_L + 45\alpha g_n \exp(\frac{5\varphi_n}{4V_T})}{12T_L + 150\alpha g_n \exp(\frac{5\varphi_n}{4V_T})}}\\
&\quad -\mathbf{J_n} \cdot \mathbf{E}. && (59)
\end{aligned}$$

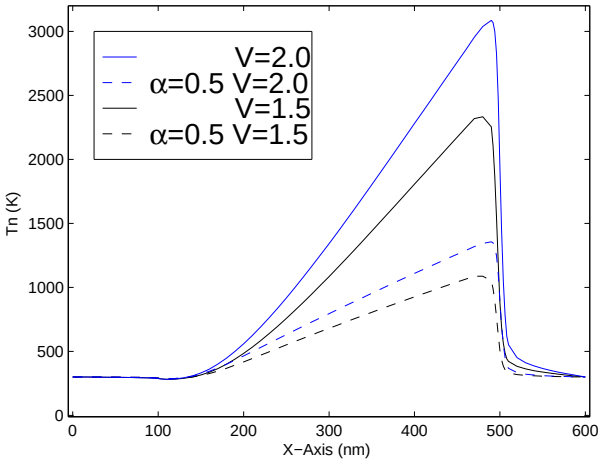

Figure 2: Electron temperature versus position in a 600 nm silicon diode.

4 Numerical Results

To demonstrate the effectiveness and accuracy of the QCET model, several numerical studies have been made for sample diode device structures with 1D and 2D cases. A benchmark device, namely, an abrupt $n^+ - n - n^+$ silicon diode is first used to verify our methods and formulation with the results reported in literature. Numerical experiments are performed first on a 600 nm silicon diode with $n^+ = 5.0 \times 10^{17} cm^{-3}$ and $n = 2.0 \times 10^{15} cm^{-3}$. The length of the n-region is approximately 400 nm. The numerical experiments for energy relaxation time are performed by employing the QCET model which is defined by (11) and (19) with non-parabolicity parameter $\alpha = 0.5$. The steady state results for this problem are illustrated by the solid and dashed curves with respective to the parabolic case and the non-parabolic case in Fig. 2. The applied voltage V_O is taken as $2.0V$ and $1.5V$. The numerical results in [6] show that the temperature is reduced due to the non-parabolicity effects. Our results agree very well with that previously reported in the paper.

To consider quantum mechanic effects including non-parabolicity, we then reduce the scale down to two cases. Case (1) is a 120 nm silicon diode with $n^+ = 5.0 \times 10^{18} cm^{-3}$ and $n = 2.0 \times 10^{15} cm^{-3}$. The length of the n-region is approximately 80 nm. The applied voltage V_O is taken as $1.2V$ and $1.0V$. Case (2) is a 30 nm silicon diode with $n^+ = 5.0 \times 10^{19} cm^{-3}$ and $n = 2.0 \times 10^{15} cm^{-3}$. The length of the n-region is approximately 20 nm. The applied voltage V_O is taken as $1.0V$ and $0.8V$. Figs. 3 and 4 show the significant change of the electron temperature predicted by the new model.

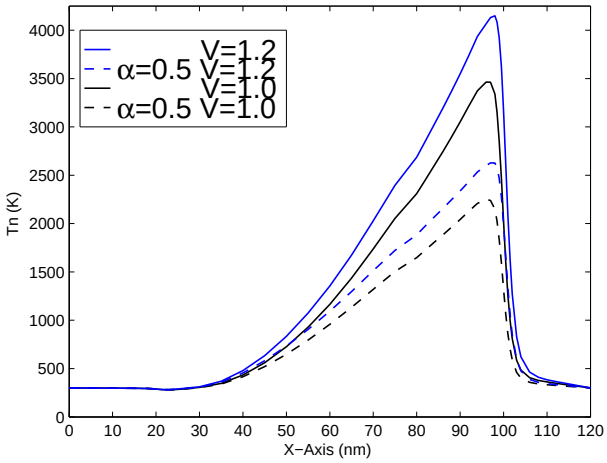

Figure 3: Electron temperature versus position in a 120 nm silicon diode.

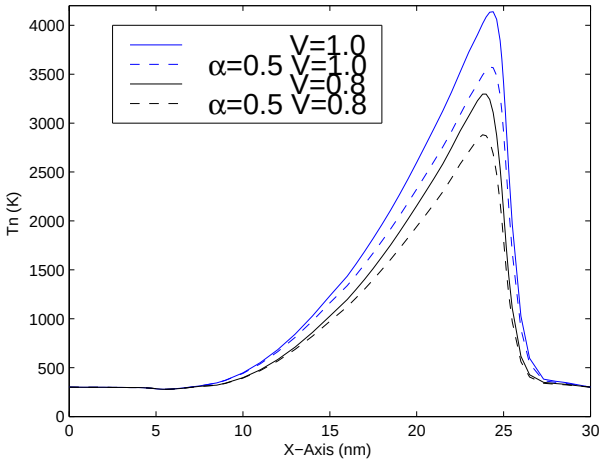

Figure 4: Electron temperature versus position in a 30 nm silicon diode.

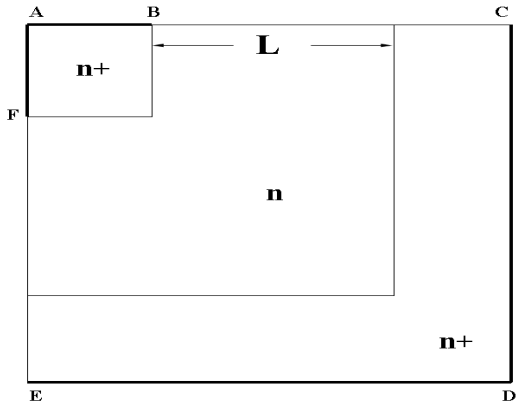

Figure 5: A 2D silicon device. Contacts are denoted by bold lines.

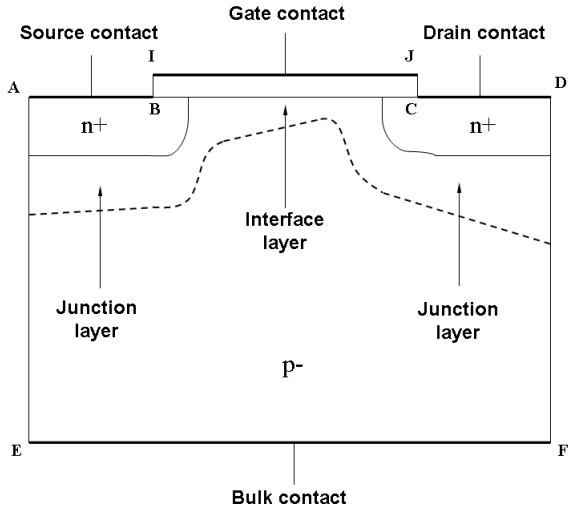

Figure 6: A 2D MOSFET device.

The next model that we have verified is a typical 2D $n^+ - n - n^+$ deep-submicron diode illustrated in Fig. 5. The bold lines indicate the contact positions [20]. Contacts A-B and A-F are terminated at a distance of $0.1\mu m$ from the top left corner. In order to simulate a realistic device, contacts are not extended to the full n^+ region near the top left corner as shown in Fig. 5. The channel length L is $0.18\mu m$. The doping profile in the highly doped regions is $5.0 \times 10^{17} cm^{-3}$ and in the lowly doped regions is $2.0 \times 10^{15} cm^{-3}$.

The applied voltage is $1.0V$. The corresponding temperature distribution for parabolic and non-parabolic models are shown in Figs. 6 and 7 respectively. Similarly, we reduce the scale down to 40 nm. The doping profile in the highly doped regions is $5.0 \times 10^{19} cm^{-3}$ and in the lowly doped regions is $2.0 \times 10^{15} cm^{-3}$. The applied voltage is $1.0V$. The corresponding temperature distribution for parabolic and non-parabolic models are shown in Figs. 8 and 9 respectively.

The third example of our simulation test on the model is a typical 2D MOSFET device structure illustrated in Fig. 10. The device has an elliptical 10^{20} cm^3 Gaussian doping profiles in the source and drain regions and 10^{16} cm^3 in the p-substrate region as shown in [21]. The junction depth is 200 nm, the lateral diffusion under gate is 80 nm and the channel length is 340 nm. With V_{BS}=0 V, V_{DS}=1.5 V, and V_{GS}=1.0 V, Figs. 11 and 12 present the electron temperature distributions for parabolic and non-parabolic models. Similarly, we reduce the channel length down to 34 nm. It has an elliptical 10^{19} cm^3 Gaussian doping profiles in the source and drain regions and 10^{16} cm^3 in the p-substrate region as shown in [9]. The junction depth is 20 nm, the lateral diffusion under gate is 8 nm. With V_{BS}=0 V, V_{DS}=1.0 V, and V_{GS}=0.8, Figs. 13 and 14 show the electron temperature distributions for parabolic and non-parabolic models. Tables 1 and 2 show results for maximal electron temperature between the parabolic and non-parabolic energy relaxation time models. The numerical results are in good agreement that the temperature is reduced due to the non-parabolicity effects.

Table 1
Maximal temperatures for two time models (diodes)

	$600nm$ (1D)		$120nm$ (1D)	
	$V = 2.0$	$V = 1.5$	$V = 1.2$	$V = 1.0$
PM	3085.9	2332.6	4149.5	3464.3
NM	1356.2	1087.2	2628.3	2250.3
	$30nm$ (1D)		$400nm$ (2D)	$40nm$ (2D)
	$V = 1.0$	$V = 0.8$	$V = 1.0$	$V = 1.0$
PM	4139.4	3296.6	2483.9	4212.5
NM	3572.7	2880.3	1171.5	3060.6

Table 2
Maximal temperatures for two time models (MOSFETs)

	$340nm$ (2D)	$34nm$ (2D)
	$V_{GS} = 1.0$	$V_{GS} = 0.8$
PM	3950.2	3645.6
NM	2729.1	2574.8

In the tables, *PM* denotes the parabolic energy relaxation time model and *NM* denotes the non-parabolic energy relaxation time model.

5 Conclusion

An extension for the QCET model to consider the non-parabolic band diagrams in the sense of Kane has been proposed. We get explicit expressions of energy

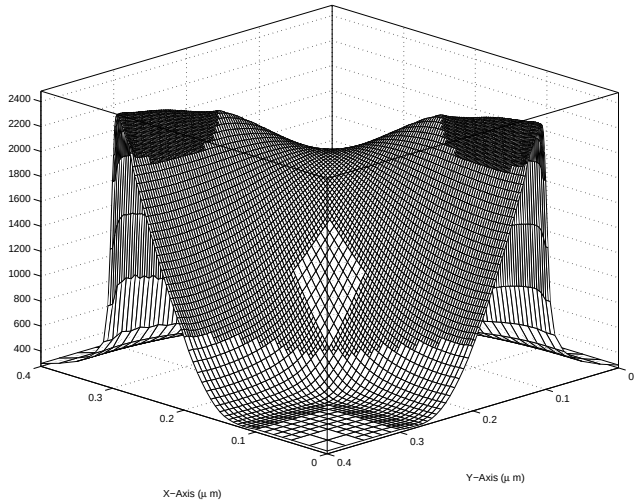

Figure 7: Electron temperature for parabolic time model in a 400 nm silicon diode.

relaxation time involving the non-parabolic band effects. There is an important parameter, namely, the non-parabolicity parameter α. Numerical simulations on diodes with the length down to 30 nm using this model have been performed. The results for 30 nm device have displayed that the electron temperature is reduced significantly from the parabolic case to the non-parabolic case. The non-parabolic effect is very important for hot-electron nano-devices and should be considered in advanced semiconductor simulation.

Acknowledgements: We are grateful to the National Center for High-performance Computing for computer time and facilities. This work was supported by NSC under Grant 100-2115-M-017-002 and 99-2115-M-134-004-MY3, Taiwan.

References:

[1] N. Caka, M. Zabeli, M. Limani and Q. Kabashi, Impact of MOSFET Parameters on its Parasitic Capacitances, *Proceedings of the 6th WSEAS Int. Conf. on Electronics, Hardware, Wireless and Optical Communications*, 2007.

[2] N. Y. A. Shammas, D. Chamund and P. Taylor, Advances in Semiconductor Devices and Their Growing Use in Electrical Circuits and Systems, *12th WSEAS International Conference on CIRCUITS*, 2008.

[3] C.-C. Wu, C.-C. Li and T.-H. Wang, Multifactor Performance Measure Model with an Application to Semiconductor industry Performance *Proceedings of the 11th WSEAS Inter-*

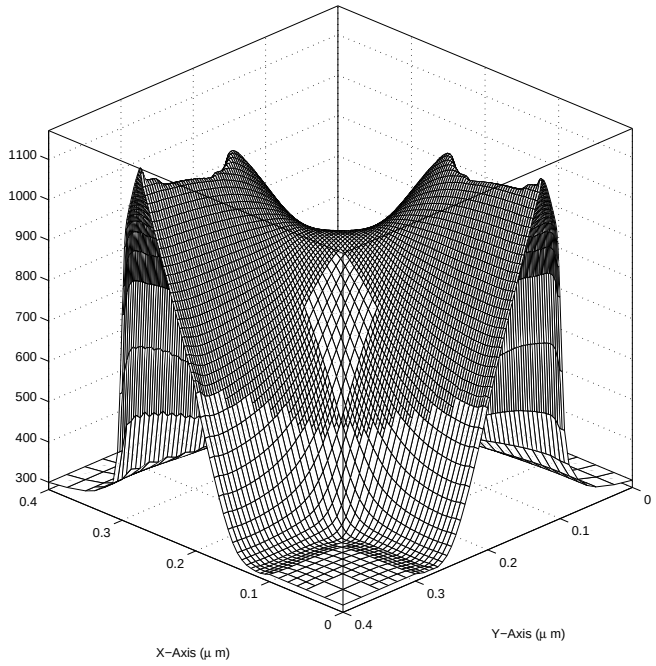

Figure 8: Electron temperature for non-parabolic time model in a 400 nm silicon diode.

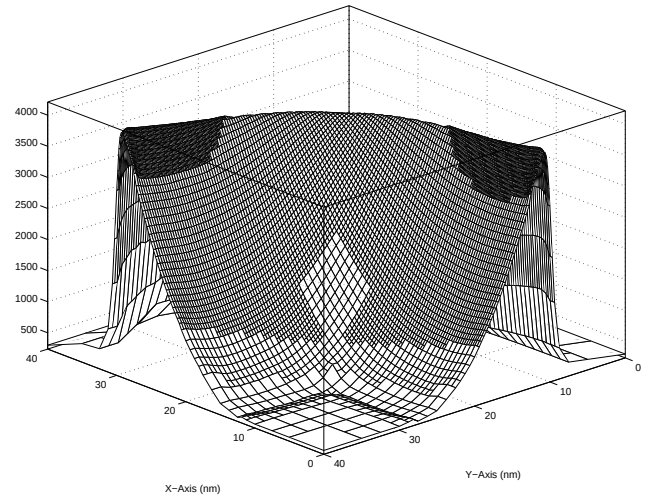

Figure 9: Electron temperature for parabolic time model in a 40 nm silicon diode.

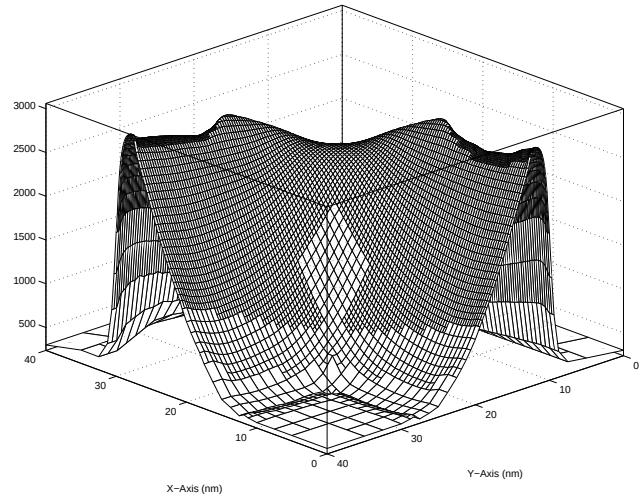

Figure 10: Electron temperature for non-parabolic time model in a 40 nm silicon diode.

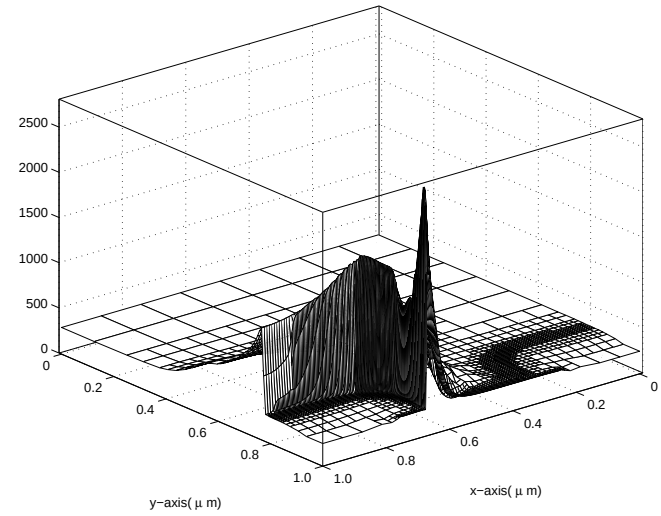

Figure 12: Electron temperature for non-parabolic time model in a 340 nm MOSFET.

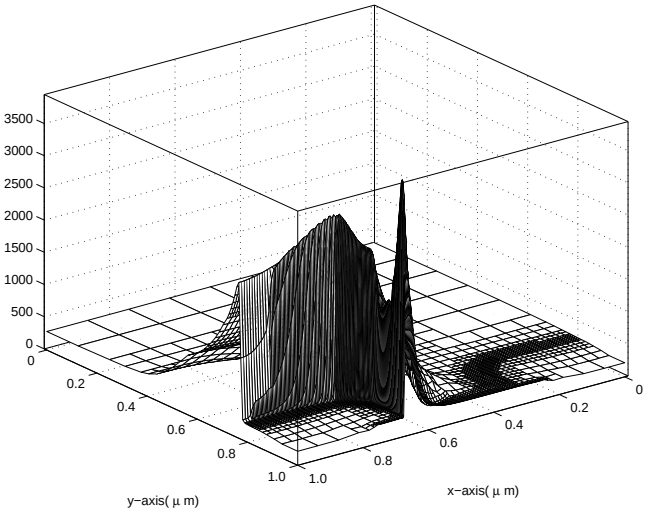

Figure 11: Electron temperature for parabolic time model in a 340 nm MOSFET.

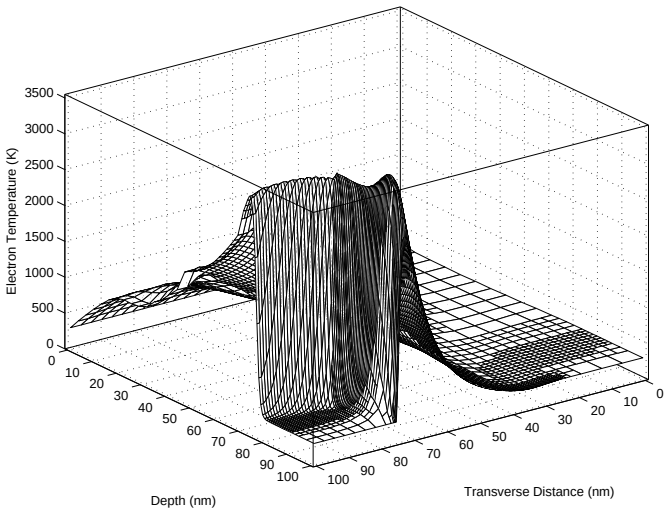

Figure 13: Electron temperature for parabolic time model in a 34 nm MOSFET.

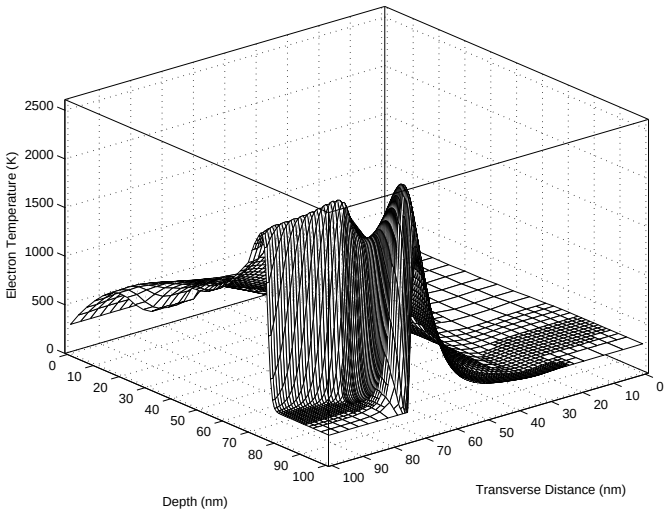

Figure 14: Electron temperature for non-parabolic time model in a 34 nm MOSFET.

national Conference on APPLIED MATHEMATICS, 2007.

[4] S. S. Attar, M.C.E. Yagoub, and F. Mohammadi, Simulation of Electro-Thermal Effects in Device and Circuit, *Proceedings of the 10th WSEAS International Conference on CIRCUITS*, 2006.

[5] P. A. Markowich, *The Stationary Semiconductor Device Equations*, Springer, 1986.

[6] P. Degond, A. Jügel and P. Pietra, Numerical Discretization of Energy-transport Models for Semiconductors with Non-parabolic Band Structure, *SIAM on Scientific Computing* Vol. 22, 2000, pp. 986–1007.

[7] D. Chen, E. Kan, U. Ravaioli, C. Shu, and R. Dutton, An Improved Energy Transport Model Including Non-parabolicity and Non-Maxwellian Distribution Effects, *IEEE Electron Device Letters* Vol. 13, 1992, pp. 26–28.

[8] E. Lyumkis, B. Polsky, A. Shur, and P. Visocky, Transient Semiconductor Device Simulation Including Energy Balance Equation, *COMPEL* Vol. 11, 1992, pp. 311–325.

[9] R.-C. Chen and J.-L. Liu, A Quantum Corrected Energy Transport Model for Nanoscale Semiconductor Devices, *J. Comput. Phys.* Vol. 204, 2005, pp. 131–156.

[10] R.-C. Chen and J.-L. Liu, An Accelerated Monotone Iterative Method for the Quantum-corrected Energy Transport Model, *J. Comput. Phys.* Vol. 227, 2008, pp. 6226–6240.

[11] M. G. Ancona, H. F. Tiersten, Macroscopic Physics of the Silicon Inversion Layer, *Phys. Rev. B* Vol. 35, 1987, pp. 7959.

[12] M. G. Ancona, G. J. Iafrate, Quantum Correction to the Equation of State of an Electron Gas in a Semiconductor, *Phys. Rev. B* Vol. 39, 1989, pp. 9536.

[13] P. Andrei, Identification Technique for the Density-gradient Model ,*4th WSEAS International Conference on ELECTRONICS, CONTROL and SIGNAL PROCESSING*, 2005, pp.132–137.

[14] R.-C. Chen, An Exponential-Fitting Method for the Quantum Corrected Equations, *Proceedings of the 11th WSEAS Int. Conf. on MATHEMATICAL METHODS, COMPUTATIONAL TECHNIQUES AND INTELLIGENT SYSTEMS*, 2009.

[15] C. L. Gardner, The Quantum Hydrodynamic Model for Semiconductor Devices, *SIAM J. Appl. Math.* Vol. 54, 1994, pp. 409.

[16] V. Chiritoiu, M. A. Mioc, M. Cristea and M. Costache, Numerical Approach in Quantum Modelling for Semiconductors *Proceedings of the 13th WSEAS International Conference on COMPUTERS*, 2009.

[17] E. Kane, Band Structure of Indium-antimonide, *J. Phys. Chem. Solids* Vol. 1, 1957, pp. 249–261.

[18] N. Ben Abdallah and P. Degond, On a Hierarchy of Macroscopic Models for Semiconductors, *J. Math. Phys.* Vol. 37, 1996, pp. 3306.

[19] G. Baccarani and M.R. Wordeman, An Investigation of Steady-state Velocity Overshoot in Silicon, *Solid-State Electron* Vol. 28, 1985, pp. 407–416.

[20] N. R. Aluru, A. Raefsky, P. M. Pinsky, K. H. Law, R. J. G. Goossens, R. W. Dutton, A Finite Element Formulation for the Hydrodynamic Semiconductor Device Equations, *Comput. Methods Appl. Mech. Engrg.* Vol. 107, 1993, pp. 269–298.

[21] R.-C. Chen and J.-L. Liu, An Iterative mMethod for Adaptive Finite Element Solutions of an Energy Transport Model of Semiconductor Devices, *J. Comput. Phys.* Vol. 189, 2003, pp. 579–606.